Available online at www.sciencedirect.com
ScienceDirect
Solar Energy Materials & Solar Cells 92 (2008) 576–580
Solar Energy Materials and Solar Cells
www.elsevier.com/locate/solmat

Microcrystalline-phase p-type a-Si:O:H windows prepared by Cat-CVD

Yasuhiro Matsumoto[a,*], Zhenrui Yu[b], R. Victor Sánchez[a]

[a]*Electrical Engineering Department, Centro de Investigación y de Estudios Avanzados del IPN, Av. IPN 2508 Colonia San Pedro Zacatenco, Mexico 07360, Mexico*
[b]*Institute of Photoelectronics, Nankai University, China*

Received 15 May 2007; received in revised form 22 October 2007; accepted 20 December 2007

Abstract

Different amounts of oxygen, boron-doped hydrogenated amorphous silicon (a-Si:H) and hydrogenated microcrystalline silicon (μc-Si:H) deposition were carried out using catalytic chemical-vapor deposition (Cat-CVD) process. Pure silane (SiH_4), hydrogen (H_2), oxygen (O_2), and diluted diborane (B_2H_6) gases were used at the deposition pressure of 0.1–0.5 Torr. The tungsten catalyst temperature (T_{fil}) was varied from 1700 to 2100 °C. Sample transmittance measurement shows an optical-band gap ($E_{g_{opt}}$) variation from 1.45 to 2.1 eV X-ray diffraction (XRD) spectra have revealed silicon microcrystalline phases for the samples prepared at the temperature greater than T_{fil}∼1900 °C. For the used silicon oxide deposition conditions, no strong tungsten filament degradation was observed after a number of sample preparations.

Keywords: Boron-doped silicon oxide; Solar cell windows; Catalytic-CVD; Microcrystalline silicon

1. Introduction

Since Carlson and Wronski have developed the first hydrogenated amorphous silicon (a-Si:H) solar cell in 1976 [1], many efforts have been done for improving its energy conversion efficiency. Beside stable and reliable intrinsic a-Si:H material research, it has been paid an especial attention on wider and higher conductive p-type window-layers. After more than two decades, boron-doped hydrogenated amorphous silicon-carbide (p-a-Si:C:H) continues as one of the best thin-film silicon-based window material [2,3].

Table 1 shows a brief synthesis for different window materials obtained for the thin-film silicon-based solar cell application. There have been different window materials mostly based on silicon-carbide by plasma-enhanced chemical-vapor deposition (PECVD), photochemical vapor deposition (Photo-CVD), electron cyclotron resonance chemical vapor deposition (ECR-CVD) and later on by catalytic chemical vapor deposition (Cat-CVD). By means of PECVD technique, Fujikake et al. obtained the hydrogenated amorphous silicon oxide (a-Si:O_x:H) using CO_2 as an oxygen source [4]. This window-layer processed in 1992, contributed with the highest conversion efficiency of 12.5% for 1 cm^2 area solar cells, and more than 10% efficiency for the correspondent $30 \times 40\,cm^2$ sub-module. In spite of these results, the a-Si:O_x:H window is still a less explored material for solar cell application.

In the other hand and more recently, there have obtained a-SiC:H by using Cat-CVD technique [5,6]. The Cat-CVD process, it takes place upon catalytic cracking of the reactant gases at the surface of a filament heated at temperatures in the range of 1500–2000 °C [7]. Cat-CVD offers several features that overcome some of the PECVD limitations, as an absence of ion bombardment during deposition, high deposition rate, and low maintenance costs. This technique has been expanding for a great variety of suitable materials for electronic device applications [8–11]. Furthermore, approaches to obtain a-Si:O_x:H deposition has been made using this technique [12,13]. Even though, there exist very scarce reports about a-Si:O_x:H materials prepared by Cat-CVD. In this work, boron-doped microcrystalline phase-involved a-Si:O_x:H

*Corresponding author. Tel.: +52 55 5061 3783; fax: +52 55 5061 3978.
E-mail address: ymatsumo@cinvestav.mx (Y. Matsumoto).

0927-0248/$ - see front matter © 2007 Elsevier B.V. All rights reserved.
doi:10.1016/j.solmat.2007.12.008

Table 1
Different p-type a-Si and μc-Si-based windows for solar cell developments

Year	Researchers	Type of material	Deposition method	Results (%)
1976	Carlson and Wronski [1]	First a-Si solar cell	Plasma-CVD	2.4
1982	Hamakawa and co-workers [2]	a-SiC	Plasma-CVD	8.0
1985	Yamada et al. [21]	a-SiC, $E_{g_{opt}} = 2.0\,eV$, $7 \times 10^{-5}\,S\,m^{-1}$	Photo-CVD	9.5
1988	Goldsteim et al. [22]	μc-SiC, $1 \times 10^{-3}\,Scm^{-1}$	Plasma-CVD	
1990	Hamakawa et al. [23]	μc-SiC, $E_{g_{opt}} = 2.1\,eV$, $10\,S\,cm^{-1}$	ECR-CVD	12.0
1992	Demichelis et al. [24]	μc-SiC, $E_{g_{opt}} = 2.1\,eV$, $1 \times 10^{-3}\,S\,cm^{-1}$	Plasma-CVD	
1992	Fujikake et al. [4]	a-SiO	Plasma-CVD, CO_2	
			Cell area $= 1\,cm^2$	12.5
			Sub-module $30 \times 40\,cm^2$	10.1
1995	Dasgupta et al. [25]	μc-SiC, $E_{04} = 2.2\,eV$, $2 \times 10^{-2}\,S\,cm^{-1}$	High power photo-CVD	
1998	Rath and Schropp [26]	μc-Si, $1.0 \times 10^{-2}\,S\,cm^{-1}$	Plasma-CVD, wide-gap solar cell	
1999	Carabe et al. [27]	μc-Si, $E_{g_{opt}} = 2.1\,eV$, $1 \times 10^{-2}\,S\,cm^{-1}$	Plasma-CVD, $B(CH_3)_3$; BF_3	
2000	Ray and Ray [28]	μc-SiO, $E_g = 1.95\,eV$, $0.22\,S\,cm^{-1}$	Photo-CVD CO_2	
2000	Jadkar et al. [29]	μc-Si, $E_{g_{opt}} = 2.0\,eV$, $0.08\,S\,cm^{-1}$	Cat-CVD	
2001	Mukherjee et al. [30]	μc-Si, $1\,S\,cm^{-1}$	Cat-CVD, $B(CH_3)_3$	
2002	Wada et al. [31]	μc-Si, carbon add, V_{oc} increment	Plasma-CVD solar cell	
2003	Chikusa et al. [32]	a-SiC, pin-type solar cell	Cat-CVD	
2004	Toyama et al. [33]	μc-SiC, $E_{04} = 2.0\,eV$, $1 \times 10^{-3}\,S\,cm^{-1}$	VHF plasma-CVD, 40 MHz, C_2H_6	
2007	Konagai [34]	μc-3C-SiC, $E_g = 2.0\,eV$, $1 \times 10^{-2}\,S\,cm^{-1}$		
2007	Itoh et al. [35]	μc-SiC, $E_{04} = 1.99\,eV$, $15.1\,S\,cm^{-1}$	Cat-CVD, SiH_3CH_3	

deposition feasibilities are presented with its correspondent electrical and optical properties.

2. Experimental development

Cat-CVD deposition system consists of stainless-steel chamber evacuated through a turbomolecular pump (Varian model V-550) with the background vacuum level of $1.0 \times 10{-}6$ Torr. First, the hydrogenated amorphous silicon oxide (a-Si:O_x:H) deposition were carried out on glass and c-Si substrates at different catalyzer and substrate temperatures using pure SiH_4, H_2, and O_2. After that, boron-doped samples were prepared using 1% diborane (B_2H_6) gas diluted in H_2. The gas sources were directed toward a 15-cm-long, 0.75-mm-diameter coiled tungsten catalyzer. The catalyzer temperature (T_{fil}) was varied from 1700 to 2100 °C and monitored by an IR detector (Chino model IR-AHS). The substrate temperature (T_{sus}) was varied form 100 to 400 °C, while the chamber pressure were controlled by a throttle valve (MKS model 253B), maintaining 0.1 Torr and the deposition time was fixed to 20 min for all the samples.

The deposited films were analyzed by the transmittance spectra (Shimadzu UV-2401PC) and Fourier transformed infrared (FTIR) spectroscopy (Thermo Nicolet model 470) with 4-cm^{-1} resolution to observe hydrogen- and oxygen-related bond natures. The thin-film structural analysis was made using X-ray diffraction spectroscopy (XRD), (Siemens D5000). Optical-band gap ($E_{g_{opt}}$) was estimated from transmittance data using Swanepoel's procedure [14]. Photo-conductivity measurements were carried out for the prepared samples using ELH halogen-lamp with dichroic reflector at 100 mW/cm^2.

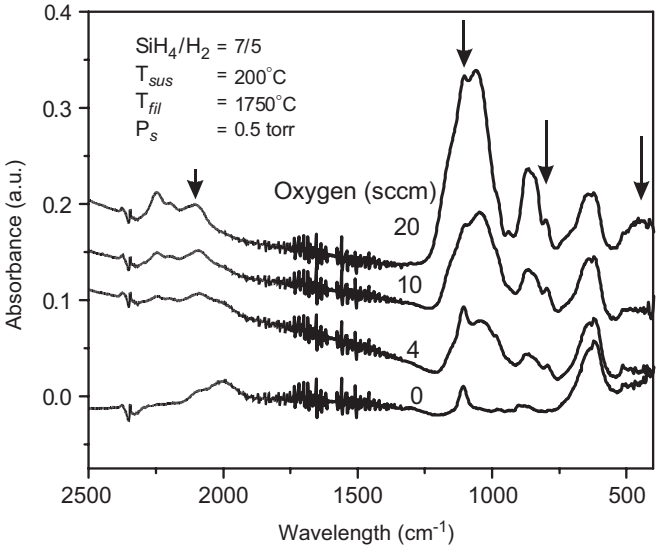

Fig. 1. FTIR spectra for the samples deposited using Cat-CVD. Oxygen incorporation is appreciated with oxygen flow increment.

3. Characterization

3.1. IR and optical characterization

Fig. 1 shows the FTIR spectra obtained from the films deposited on c-Si substrates at the chamber pressure (P_s) of 0.5 Torr, $SiH_4 = 7$ and $H_2 = 5$ standard cubic centimeter per minute (SCCM) for different oxygen flow at T_{fil} and T_{sus} of 1750 and 200 °C, respectively. In general, the obtained spectra resemble to a-Si:O_x:H films that obtained by means of PECVD technique, which is widely discussed by different authors [15–17]. In Fig. 1, the corresponding

oxygen-related IR-absorption spectra are indicated by the downward directed arrows. As can be seen, all of the observed oxygen-related spectra increase, indicating that the oxygen concentration in the films is augmented by oxygen flow increment. The absorption peaks placed on 480, 800 (the small peak), and 1050 cm^{-1} correspond to the rocking, bending, and stretching modes, respectively, while 2090 cm^{-1} absorption correlates the Si–H bond-stretching vibration of monohydrade phase [18].

Notice that IR spectra of the sample prepared without oxygen flow shows Si–O related peak at 1108 cm^{-1}, which is probably due to c-Si bulk-related oxygen.

For the samples prepared without diborane doping, the $E_{g_{opt}}$ reaches the maximum value of about 2.1 eV at $O_2 = 20$ SCCM (not shown in this work). Furthermore, for the sample prepared at $T_{fil} = 1950\,^{\circ}C$, the corresponding $E_{g_{opt}}$ achieved wider value of about 2.70 eV at the same 20 SCCM oxygen flow [19].

4. Results and discussion

Fig. 2 shows the characteristics of the prepared boron-doped samples for the $E_{g_{opt}}$, conductivity (σ), and its deposition rate (d_r). The p-a-Si:O:H films were prepared at different tungsten catalyst temperature (T_{fil}) with the substrate temperature (T_{sus}) of 200 °C, deposition chamber pressure (P_s) of 0.1 Torr, SiH_4:H_2:O_2 fixed all to 5 SCCM and B_2H_6 to 10 SCCM. As can be seen, when T_{fil} increases from 1700 to 2100 °C, the d_r and σ tends to increase, while the $E_{g_{opt}}$ has an "U"-shaped tendency with the lowest $E_{g_{opt}}$ at $T_{fil} = 1850\,^{\circ}C$. For lower catalyst temperature of 1700 °C, the maximum optical-band gap were 1.87–1.93 eV with σ of 1.0×10^{-8}–$5.0 \times 10^{-7}\,\Omega^{-1}\,cm^{-1}$. The maximum $E_{g_{opt}}$ of 1.98 eV was obtained at $T_{fil} = 2050\,^{\circ}C$, σ of about $4 \times 10^{-4}\,\Omega^{-1}\,cm^{-1}$ with the deposition rate of 0.48 nm/s. The best conductivity σ of $1.0 \times 10^{-2}\,\Omega^{-1}\,cm^{-1}$ was achieved at $T_{fil} = 1950\,^{\circ}C$ with its corresponding $E_{g_{opt}}$ of 1.82–1.88 eV. The steep conductivity increment above $T_{fil} = 1900\,^{\circ}C$ is due to the silicon microcrystallization in the a-Si:O:H matrix as is described by XRD spectra inset in Fig. 1. The given XRD peak shows an ordinary preferential silicon grain orientation.

Fig. 3 shows $E_{g_{opt}}$, σ, and d_r for the samples deposited at $T_{fil} = 1950\,^{\circ}C$, $P_s = 0.1$ Torr at different T_{sus}. The source gases flow were the same as the samples prepared previously. As can be seen, when the T_{sus} increases from

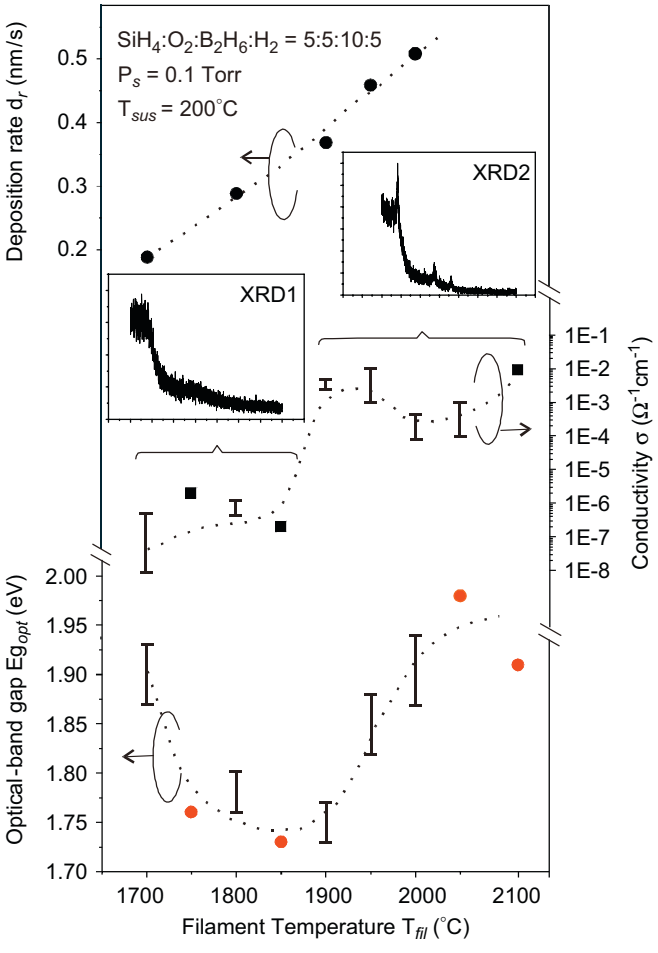

Fig. 2. Optical-band gap ($E_{g_{opt}}$), electrical conductivity (σ), and deposition rate (d_r) for the samples prepared at different tungsten catalyst temperature (T_{fil}).

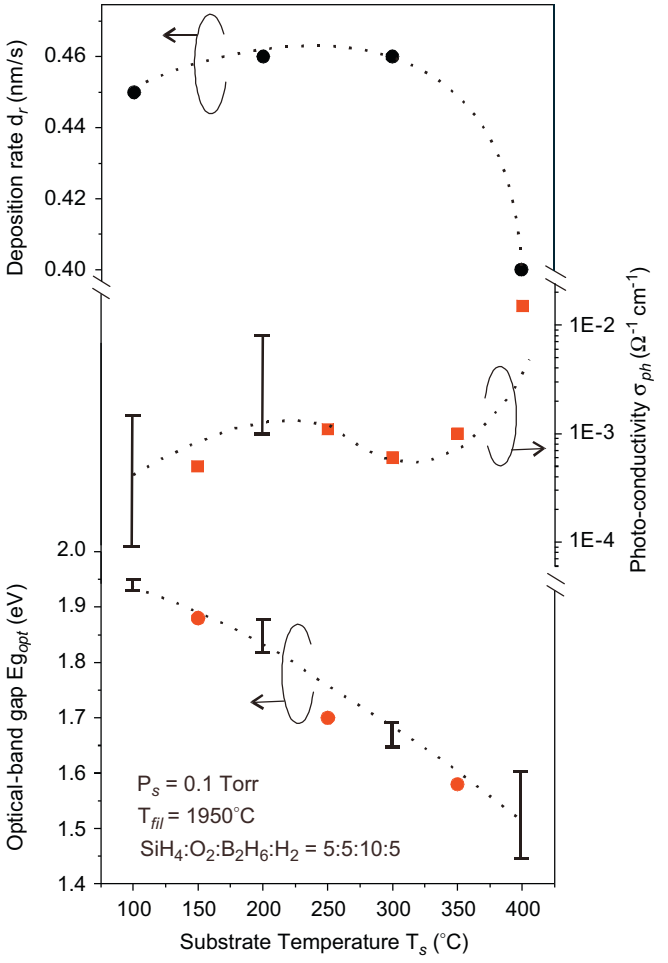

Fig. 3. $E_{g_{opt}}$, σ, and d_r for the samples deposited at $T_{fil} = 1950\,^{\circ}C$, $P_s = 0.1$ Torr at different substrate temperature (T_{sus}) of 100–400 °C.

100 to 400 °C, the $E_{g_{opt}}$ decreases steeply from 1.93 to 1.45 eV, but the conductivity tends to remain with certain fluctuations. The sample deposited at $T_{sus} = 100$ °C, its final temperature increases to 146 °C after 20 min due to the catalyst thermal induction. This sample with $E_{g_{opt}} = 1.93$ and $\sigma = 1.5 \times 10^{-3}\,\Omega^{-1}\,cm^{-1}$, could be as a candidate for the solar cell window material. The correspondent deposition rate was $d_r = 0.45$ nm/s.

Fig. 4 shows electrical conductivity and its corresponding $E_{g_{opt}}$ values for the samples prepared at constant SiH_4 and H_2 flow of 5 SCCM. The B_2H_6 flow was varied from 5 to 15 SCCM and the O_2 flow was settled for 5 and 10 SCCM. The T_{fil}, P_s, and T_{sus} were 1950 °C, 0.1 Torr, and 200 °C, respectively. As can be seen, the sample conductivity increases with the B_2H_6 flow increment, which means boron incorporation. However, as is expected, the $E_{g_{opt}}$ decreases with the diborane flow. The sample prepared at the maximum B_2H_6 flow with O_2 flow of 5 SCCM, remains its optical-band gap of 1.79 eV and conductivity of about $0.02\,\Omega^{-1}\,cm^{-1}$. The sample deposited with 10 SCCM O_2 flow and at the same diborane flow ratio, the $E_{g_{opt}}$ increases to 1.90 eV due to greater oxygen incorporation in the deposited film, while its σ reduces to $5.1 \times 10^{-5}\,\Omega^{-1}\,cm^{-1}$. Even though, this material also could be another candidate for thin-film solar cell window-layer.

For the samples prepared at diborane and oxygen flow of 5 SCCM, the optical-band gap achieves above 2.05 eV,

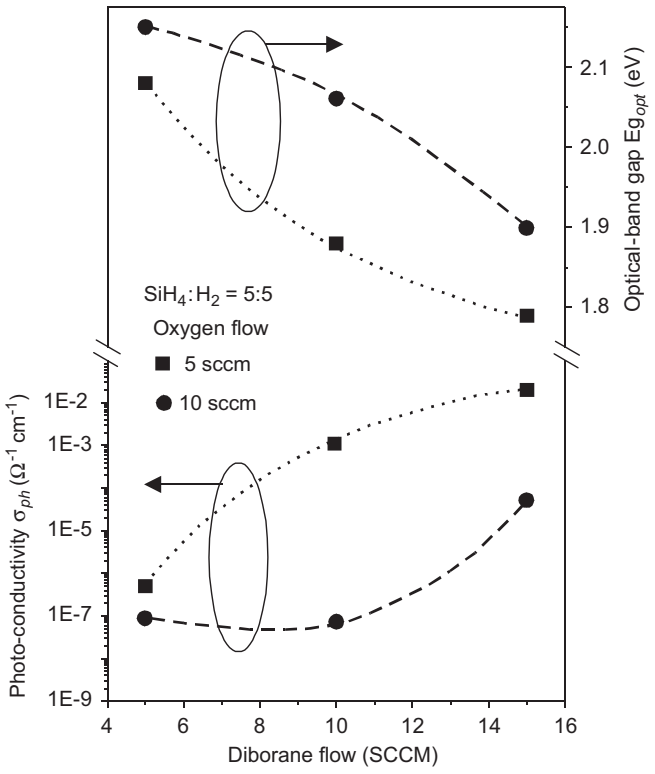

Fig. 4. Optical-band gap $E_{g_{opt}}$ and its corresponding electrical conductivity values for the samples prepared with different amount of diborane concentration. A constant SiH_4 and H_2 flow of 5 SCCM, and two different amount of oxygen flow were considered.

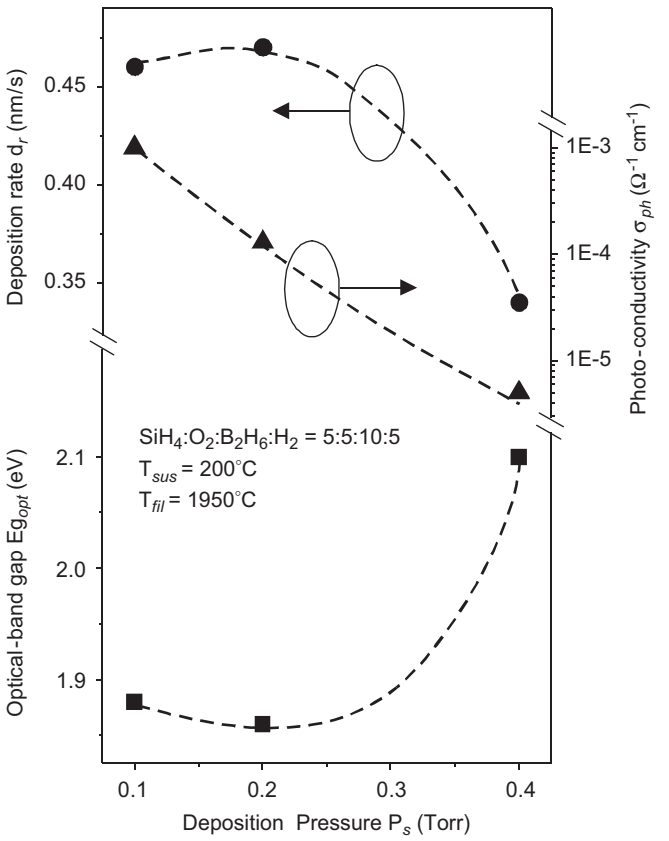

Fig. 5. Optical-band gap and conductivity for the samples prepared at different deposition chamber pressure.

but with only σ of about $5.0 \times 10^{-7}\,\Omega^{-1}\,cm^{-1}$, which has to be improved. The deposition rate of the sample was 0.41–0.57 nm/s (not shown in the figure).

Fig. 5 shows optical and electrical properties of a p-type a-Si:O_x:H as a function of deposition pressure (P_s). The P_s was varied in the 0.1–0.4 Torr interval with constant flow for SiH_4, H_2, O_2, of 5 SCCM, B_2H_6 of 10 SCCM, $T_{fil} = 1950$ °C, and $T_{sus} = 200$ °C. The $E_{g_{opt}}$ has a tendency to grow as P_s increases, but σ decreases. The maximum achieved $E_{g_{opt}}$ was 2.1 eV at 0.4 Torr with its conductivity $\sigma = 5.0 \times 10^{-6}\,\Omega^{-1}\,cm^{-1}$ with the deposition rate of about 0.34 nm/s. This value, also have suitability for thin-film solar cell window-layer application.

For the used Cat-CVD deposition condition, the detected tungsten filament degradation was found as normally occurs in a-Si:H deposition, and no accelerated degradation were observed due to the possible corrosion reactions. The H_2 injection in Cat-CVD deposition system, may contribute to avoid the direct oxygen reaction at the filament surface. As is ascribed by Hickmott, the kinetic process at the surface of the filament depends on the rates of chemisorptions, surface diffusion, and evaporation of the molecular and atomic hydrogen production ratio [20]. So, if the hydrogen component at the filament surface is more active than that of oxygen, there may reduce the oxygen direct interaction.

5. Conclusions

p-Type a-Si:O_x:H and μc-Si:O_x:H films have been obtained using pure silane, hydrogen, oxygen, and diluted diborane by means of Cat-CVD technique. Optical and electrical properties as a function of substrate temperature, catalyst temperature, deposition pressure, and boron doping ratio were elucidated. Different amount of boron and oxygen incorporation were confirmed by electrical conductivity and FTIR measurements, respectively.

The best p-type μc-Si:O_x:H material having $E_{g_{opt}}$ of 1.98 eV, with the conductivity of about $4 \times 10^{-4}\,\Omega^{-1}\,cm^{-1}$ was obtained for $T_{fil} = 2050\,^{\circ}C$, $T_{sus} = 200\,^{\circ}C$ and the deposition rate of 0.48 nm/s. For samples prepared at $T_{fil} = 1950\,^{\circ}C$ with the substrate temperature of 100–146 °C was $E_{g_{opt}}$ of 1.93 eV, and $\sigma \sim 1.5 \times 10^{-3}\,\Omega^{-1}\,cm^{-1}$ with 0.45 nm/s deposition rate has been obtained. These prepared samples could be as a thin-film solar cell window-layer application candidate.

The tungsten catalyst had a similar degradation as that observed in a-Si:H film deposition for the used processes conditions.

Acknowledgments

The authors thank Gabriela López for sample preparations and its optical characterization. The authors are indebted to Gerardo Francisco Pérez for FTIR measurements, Miguel Angel Luna for sample thickness measurements, Martín Jiménez for the technical support and also indebted with Ms. Marcela Guerrero of Physics Department for the XRD measurements.

References

[1] D.E. Carlson, C.R. Wronski, Appl. Phys. Lett. 29 (1976) 602.
[2] Y. Tawada, K. Tsuge, M. Kondo, H. Okamoto, Y. Hamakawa, J. Appl. Phys. 31 (1982) 5273.
[3] Z. Yu, I. Pereyra, M.P. Carreno, Sol. Energy Mater. Sol. Cells 66 (2001) 155.
[4] S. Fujikake, et al., Mater. Res. Soc. Symp. Proc. 258 (1992) 875.
[5] T. Itoh, et al., Thin Solid Films 395 (2001) 240.
[6] I. Ferreira, et al., Appl. Surf. Sci. 184 (2001) 8.
[7] H. Matsumura, Jpn. J. Appl. Phys. 30 (1991) L1522.
[8] A.H. Mahan, R.E.I. Schropp, J.P. Conde, H. Matsumura, M.B. Schubert, Proceedings of the First International Conference on Cat-CVD (Hot-wire CVD) Process, Elsevier, Amsterdam, 2000.
[9] A. Madan, S. Morrison, Sol. Energy Mater. Sol. Cells 55 (1998) 127.
[10] J.K. Rath, Sol. Energy Mater. Sol. Cells 76 (2003) 431.
[11] A.H. Mahan, Sol. Energy Mater. Sol. Cells 78 (2003) 299.
[12] K. Saito, et al., Thin Solid Films 430 (2003) 287.
[13] K. Yasuhiro Matsumoto, L. Mauricio Ortega, T. Juan-Manuel Peza, B. Mario-Alfredo Reyes, E. Arturo Escobosa, Thin Solid Films 490 (2005) 173.
[14] R. Swanepoel, J. Phys. E: Sci. Instrum. 16 (1983) 1214.
[15] G. Lucovsky, Solid State Commun. 29 (1979) 571.
[16] L. He, T. Inokuma, Y. Kurata, S. Hasegawa, J. Non-Cryst. Solids 185 (1995) 249.
[17] C.T. Kirk, Phys. Rev. B 38 (1988) 1225.
[18] P.G. Pai, S.S. Chao, Y. Takagi, G. Lucovsky, J. Vac. Sci. Technol. A4 (3) (1986) 689.
[19] Y. Matsumoto, M.A. Reyes, A. Escobosa, J. Appl. Phys. 98 (2005) 014909.
[20] T.W. Hickmott, J. Chem. Phys. 32 (1960) 810.
[21] A. Yamada, J. Kenne, M. Konagai, K. Takahashi, Appl. Phys. Lett. 46 (3) (1985) 272.
[22] B. Goldsteim, C.R. Dickson, I.H. Campvell, P.M. Fauchet, Appl. Phys. Lett. 53 (26) (1988) 2672.
[23] Y. Hamakawa, Y. Matsumoto, G. Hirata, H. Okamoto, Proceedings of Materials Research Society Symposium, Boston, vol. 164, 1990, pp. 291–301.
[24] F. Demichelis, C.F. Pirri, E. Tresso, J. Appl. Phys. 72 (4) (1992) 1327.
[25] A. Dasgupta, S. Ghosh, S. Ray, J. Mater. Sci. Lett. 14–15 (1995) 1037.
[26] J.K. Rath, R.E.I. Schropp, Sol. Energy Mater. Sol. Cells 53 (1998) 189.
[27] J. Carabe, J.J. Gandia, N. Gonzalez, M.T. Gutierrez, Sol. Energy Mater. Sol. Cells 57 (1999) 97.
[28] T. Ray, S. Ray, Thin Solid Films 376 (2000) 241.
[29] S.R. Jadkar, J.V. Sali, M.G. Takwale, D.V. Musale, S.T. Kshirsagar, Sol. Energy Mater. Sol. Cells 64 (2000) 333.
[30] C. Mukherjee, U. Weber, H. Seitz, B. Schroder, Thin Solid Films 395 (2001) 310.
[31] T. Wada, M. Kondo, A. Matsuda, Sol. Energy Mater. Sol. Cells 74 (2002) 533.
[32] K. Chikusa, K. Takemoto, T. Itoh, N. Yoshida, S. Nonomura, Thin Solid Films 430 (2003) 245.
[33] T. Toyama, Y. Nakano, T. Ichihara, H. Okamoto, J. Non-Cryst. Solids 338–340 (2004) 106.
[34] M. Konagai, Thin Solid Films 516 (2008) 490.
[35] T. Itoh, T. Kawasaki, Y. Takai, N. Yoshida, S. Nonomura, Thin Solid Films 516 (2008) 641.